Volume 22
Number 5
March 2, 1983

Inorganic Chemistry

Contribution from the Department of Chemistry,
The Ohio State University, Columbus, Ohio 43210

Electrochemistry of Oxygen Reduction. 4. Oxygen to Water Conversion by Iron(II) Tetrakis(*N*-methyl-4-pyridyl)porphyrin via Hydrogen Peroxide

PAUL A. FORSHEY and THEODORE KUWANA*

Received April 19, 1982

The reduced form of iron tetrakis(*N*-methyl-4-pyridyl)porphyrin, electrogenerated at a highly polished glassy-carbon electrode, has been shown to be capable of reducing molecular oxygen to water via a multistepped mechanism. The electrode potential of this electrocatalysis coincided closely with the redox potential of the iron porphyrin through the pH range of 1–13. The magnitude of the catalytic current and hence the extent of oxygen reduction was found to be highly dependent on the iron porphyrin to oxygen concentration ratio. Controlled-potential coulometry with a thin-layer cell containing iron porphyrin and oxygen confirmed the ability of the ferrous form of the water-soluble porphyrin to reduce oxygen quantitatively to water. An assumption was made that the oxygen reduction proceeded through hydrogen peroxide that was either removed by disproportionation or via direct reduction by the ferrous porphyrin. The mechanistic aspects were tested by examining the removal rate of hydrogen peroxide by both the ferric and the ferrous forms of the porphyrin. The results showed that hydrogen peroxide reacted with the ferric form relatively slowly in acidic solutions while the ferrous porphyrin reacted rapidly, thereby making possible the oxygen to water conversion.

Introduction

In previous publications[1-4] the electrogenerated ferrous form of the water-soluble iron(III) tetrakis(*N*-methyl-4-pyridyl)-porphyrin pentakis(bisulfate) (abbreviated $Fe^{III}TMPyP$) has been shown to be an effective catalyst for the reduction of molecular oxygen. The catalyzed reduction with this porphyrin is unique since most of the metal macrocyclic compounds are water insoluble and, hence, are either adsorbed on or incorporated into the electrode surface.[5-18] Aside from problems of reproducibility and stability with these insoluble macrocycles, it has been difficult to identify the chemical species and the mechanistic pathway(s) involving the catalyst with oxygen.

We have found that the ferric and ferrous forms of FeTMPyP with chloride or sulfate as counterions are water soluble over a wide range of pH values without any evidence of significant surface adsorption on Pt, Au, or highly polished glassy-carbon surfaces.[15] Thus, the reaction of electrogenerated $Fe^{II}TMPyP$ with oxygen is a homogeneous reaction, permitting the electrochemical response of the electrode and the catalyst, with or without oxygen, to be studied independently. Another advantage of this porphyrin is that it can be readily synthesized and purified.[19-21]

Previous results have led us to suggest that oxygen was reduced by FeTMPyP following an EC catalytic regeneration mechanism[1] (eq 1 and 2), where reaction 2 reflected the

$$\text{E step: } Fe^{III}TMPyP + e^- = Fe^{II}TMPyP \quad (1)$$

$$\text{C step: } 2Fe^{II}TMPyP + O_2 + 2H^+ = 2Fe^{III}TMPyP + H_2O_2 \quad (2)$$

stoichiometry of oxygen being reduced to hydrogen peroxide. Although we shall see herein that oxygen can be quantitatively reduced to water using FeTMPyP, a feature of this EC mechanism is that the iron porphyrin must be in the reduced ferrous state before any reaction with oxygen can take place. Therefore, the electrode potential must be sufficiently near the redox potential of the $Fe^{III/II}TMPyP$ couple to generate at least a small concentration of $Fe^{II}TMPyP$ before oxygen reduction can be observed. A discussion of such potential dependence is often absent from reports involving surface-adsorbed catalysts because of the difficulty in determining their redox potentials.

(1) Fujihira, M; Sunakawa, K.; Osa, T. Kuwana, T. *J. Electroanal. Chem. Interfacial Electrochem.* **1978**, *88*, 299.
(2) Bettelheim, A.; Kuwana, T. *Anal. Chem.* **1979**, *51*, 2257.
(3) Bettelheim, A.; Chan, R. J. H.; Kuwana, T. *J. Electroanal. Chem. Interfacial Electrochem.* **1979**, *99*, 391.
(4) Bettelheim, A.; Chan, R. J. H.; Kuwana, T. *J. Electroanal. Chem. Interfacial Electrochem.* **1980**, *110*, 93.
(5) Jasinski, R. *J. Electrochem. Soc.* **1965**, *112*, 526.
(6) Kozawa, A.; Zilionis, V. E.; Brodd, R. J. *J. Electrochem. Soc.* **1970**, *117*, 1470.
(7) Janke, H.; Schoenborn, M.; Zimmerman, G. *Katal. Phthalocyaninen, Symp.* **1973**, 71–89.
(8) Bogdanovshaya, V. A.; Tarasevich, M. R. *Elektrokhimiya* **1975**, *11*, 914.
(9) Alferov, G. A.; Sevast'yanov, V. I. *Elektrokhimiya* **1975**, *11*, 827.
(10) Yeager, E. *NBS Spec. Publ. (U.S.)* **1976**, *No. 455*, 203–219.
(11) Collman, J. P.; Marrocco, M.; Denisevich, P.; Koval, C.; Anson, F. C. *J. Electroanal. Chem. Interfacial Electrochem.* **1979**, *101*, 117.
(12) Kolpin, C. F.; Swofford, H. S., Jr. *Anal. Chem.* **1978**, *50*, 920.
(13) Kobayashi, N.; Fujihira, M.; Sunakawa, K.; Osa, T. *J. Electroanal. Chem. Interfacial Electrochem.* **1979**, *101*, 269.
(14) Kobayashi, N.; Fujihira, M.; Matsue, T.; Osa, T. *J. Electroanal. Chem. Interfacial Electrochem.* **1979**, *103*, 427.
(15) Forshey, P. A.; Kuwana, T. *Inorg. Chem.* **1981**, *20*, 693.
(16) Collman, J. P.; Denisevich, P.; Konai, Y.; Marrocco, M.; Koval, C.; Anson, F. C. *J. Am. Chem. Soc.* **1980**, *102*, 6027.
(17) Zagal, J.; Bingra, P.; Yeager, E. *J. Electrochem. Soc.* **1980**, *127*, 1506.
(18) Behret, H.; Binder, H.; Stanstede, G.; Schrer, G. G. *J. Electroanal. Chem. Interfacial Electrochem.* **1981**, *117*, 29.
(19) Fleischer, E. B.; Hambright, F. *Inorg. Chem.* **1970**, *9*, 1757.
(20) Toppen, D. L.; Harris, F. L. *Inorg. Chem.* **1978**, *17*, 71.
(21) Pasternack, R. F.; Malek, P.; Spencer, C. *J. Inorg. Nucl. Chem.* **1977**, *39*, 1865.

0020-1669/83/1322-0699$01.50/0

Earlier cyclic voltammetric (CV) and rotating ring-disk electrode (RRDE) results[1,2] indicated that, when the $Fe^{III}TMPyP$ and oxygen concentrations were comparable at 2×10^{-4} M, hydrogen peroxide appeared to be the main product of the oxygen electrocatalytic reduction. The rate constant of reaction 1 was evaluated to be 5.8×10^{-3} cm/s in dilute sulfuric acid solutions at a highly polished glassy-carbon electrode. The rate constant of reaction 2 was estimated to be on the order of 10^7 M^{-1} s^{-1} as determined by RRDE experiments at pH 9. Both rate constants are relatively large.

The transfer of the homogeneous EC catalysis to a heterogeneous one can be accomplished, as previously demonstrated by Bettelheim et al.,[4] by immobilizing an iron porphyrin in a polymeric matrix and affixing the polymer onto a glassy-carbon surface. The extent of the oxygen reduction appeared to be dependent on the amount of iron porphyrin incorporated into the polymer. That is, at low amounts of ca. 5×10^{-11} mol/cm^2, the analysis[4] of the CV current–potential (i–E) wave height suggested hydrogen peroxide as the product, whereas at higher amounts of 5×10^{-9} mol/cm^2, an overall four-electron process converting oxygen to water appeared to occur. The present study is directed toward addressing this dependence of oxygen reduction on the concentration of the iron porphyrin. Also, an important question probed herein is the mechanistic pathway whereby a one-electron reducing agent, $Fe^{II}TMPyP$, can convert oxygen to hydrogen peroxide and then hydrogen peroxide to water (with the assumption that hydrogen peroxide is the initial oxygen reduction product) rapidly.

The experimental approach will utilize CV and controlled-potential thin-layer electrochemical methods to ascertain the concentration dependence and the extent of oxygen reduction with FeTMPyP. The question of hydrogen peroxide removal will consider the possibility of peroxide disproportionation by both oxidation states of FeTMPyP and the "direct" reduction of peroxide by electrogenerated $Fe^{II}TMPyP$. Finally, computer-calculated CV i–E curves derived from the modeling of an EC catalytic mechanism with experimentally determined kinetic values will be compared to the experimental ones.

Experimental Section

Samples of $Fe^{III}TMPyP$ were synthesized according to two different procedures. For the procedure described by Fleischer and Hambright,[19] the tetrapyridylporphyrin was methylated with use of neat dimethyl sulfate rather than methyl iodide or methyl tosylate, and the metalation involved iron as $Fe(ClO_4)_2 \cdot 6H_2O$. Crude $Fe^{III}TMPyP$ was precipitated as the perchlorate salt and repeatedly recrystallized from hot distilled water. The perchlorate salt of $Fe^{III}TMPyP$ (sample A) could be ion exchanged to obtain the chloride salt. Elemental analysis of sample A gave a ratio of 44.9:7.7:1 compared to the theoretical ratio of 44:8:1 for the elements of carbon, nitrogen, and iron, respectively. The second sample of $Fe^{III}TMPyP$ was prepared according to the procedure described by Toppen and Harris.[20] The starting material of *meso*-tetrakis(4-pyridyl)porphyrin (abbreviated TPyP) was purchased from Strem Chemical Co. and used without further purification. Methylation was accomplished by the reaction of TPyP with methyl *p*-toluenesulfonate in DMF. After metalation, with $Fe(ClO_4)_2 \cdot 6H_2O$, sodium perchlorate was added and the solution was chilled in an ice bath to precipitate the perchlorate salt of $Fe^{III}TMPyP$. The precipitate was washed with absolute ethanol and dried in a vacuum desiccator (sample B).

For an assessment of the extent of methylation, infrared (IR) spectra of $Fe^{III}TMPyP$ and the nonmethylated $Fe^{III}TPyP$ were compared to those of the reference compounds 4-*tert*-butylpyridine (Coblentz spectrum 6767) and *N*-methyl-3-carbazoylpyridinium 4-toluenesulfonate (Colblentz spectrum 2283, published by Sadtler Research Laboratories). The 1600-cm^{-1} region, characteristic of the –C=N– stretch of pyridine, shifts to larger wavenumbers, 1640–1660 cm^{-1}, upon methylation. Thus, the presence of nonmethylated pyridine appears as a shoulder on the 1640–1660-cm^{-1} band. Sample A contained less than 5% of nonmethylated pyridine whereas the amount in sample B was less than 0.5%. The extent of methylation is important since the nonmethylated compound, $Fe^{III}TPyP$, is insoluble in neutral and basic solutions and may adsorb on the electrode surface. If any iron porphyrin is adsorbed and acts as a catalyst for oxygen reduction, the results of the homogeneous EC reaction may be compromised. On the other hand, the non-methylated compounds could be either tri- or dimethylated porphyrins in which case water solubility may not be seriously affected. Certain CV experiments were repeated with both samples A and B, and the results were in good agreement within experimental error.

All other chemicals were analytical grade, and solutions were prepared with water that was deionized and then distilled in an all-glass still. A Corning Model 7 pH meter equipped with a Sargent-Welch combination glass electrode, Model S-30070-10, was used to measure pH. Nitrogen, 99.9% pure, was passed over hot copper turnings and then used for deoxygenation purposes. Oxygen concentrations were calculated on the assumption that (a) the concentration varied linearly with the partial pressure of oxygen; (b) air was composed of 20.9% oxygen; and (c) air-saturated solutions contained 2.4×10^{-4} M oxygen. Literature values[22,23] for air-saturated solutions ranged from 2.2×10^{-4} to 2.6×10^{-4} M. The concentration of $Fe^{III}TMPyP$ was determined by diluting samples of the porphyrin solution with 0.05 M H_2SO_4 and then measuring the absorbance at the 400-nm maximum with use of a molar extinction coefficient[21,24] of 1.05×10^5 M^{-1} cm^{-1}. The concentration of the hydrogen peroxide stock solution was determined by titration with standard potassium permanganate.[25]

Samples of glassy carbon, used as a working electrode, were obtained from Tokai Ltd., Atomergic Chemical, and Sigma. Electrode pretreatment consisted of polishing with alumina and felt pads (Buehler) on a Harrick (Harrick Scientific Corp., Ossining, NY) optical flat until a mirrorlike finish was obtained. The final polish was performed with 0.05-μm particle size alumina.[26] The electrodes were washed with 0.05 M H_2SO_4 and distilled water to remove residual alumina. Electrodes were used immediately after polishing. If stored, the electrodes were repolished before use according to the final polishing procedures just described.

Cyclic voltammetry and coulometry were performed with the use of a three-electrode cell in which the glassy-carbon disks were affixed to the central compartment via a neoprene O-ring gasket and a Lucite backing plate. The electrode area exposed to the solutions was 0.39 ($\pm$0.01) cm^2 unless otherwise indicated. A platinum wire, used as the auxiliary electrode, was isolated from the main compartment by a medium-density glass frit.

The reference electrode assembly for the voltammetry cell included a Luggin capillary, which was fixed in position approximately 2 mm from the center of the working electrode. A silver/silver chloride (1.0 M KCl) reference electrode was used for voltammetric experiments. Potentials in the text are reported with respect to a normal hydrogen electrode by adding +0.226 V to the observed potential. Experiments were conducted at room temperature, 21 ($\pm$2) °C.

Electrochemistry was conducted with the use of a conventional three-electrode potentiostat. The rise time of the potentiostat was less than 20 μs. Wave forms to the potentiostat were generated by a Princeton Applied Research Corp. Model 175 universal programmer.

Ultraviolet and visible spectra were determined with the use of either a Cary 15 spectrophotometer or a minicomputer-controlled rapid-scanning spectrophotometer.[27,28] Stopped-flow experiments were conducted with an Aminco-Morrow instrument. Absorbance vs. time plots were recorded by either a strip chart recorder or a Tektronix Model 7613 memory oscilloscope, depending on the time scale of the experiment.

Spectroelectrochemistry was conducted with the use of an airtight, optically transparent, thin-layer cell (OTTLE) constructed with a gold minigrid working electrode sandwiched between two plates.[29,30] One

(22) Gubbins, K.; Walker, R. *J. Electrochem. Soc.* **1965**, *112*, 469.
(23) Seidell, A. "Solubilities of Inorganic and Metal Organic Compounds", 3rd ed.; Van Nostrand: New York, 1940; Vol. 1, p 1352.
(24) Wilson, G. S.; Neri, B. P. *Ann. N.Y. Acad. Sci.* **1973**, *206*, 568.
(25) Schumb, W. C.; Satterfield, C. M.; Wentworth, R. L. "Hydrogen Peroxide"; American Chemical Society: Washington, DC, 1955; ACS Monogr. No. 128.
(26) For a description of polishing procedures, see: Evans, J. F.; Kuwana, T. *Anal. Chem.* **1979**, *51*, 358.
(27) Strojek, J. W.; Gruver, G. A.; Kuwana, T. *Anal. Chem.* **1969**, *41*, 487.
(28) Szentirmay, R.; Kuwana, T. *Anal. Chem.* **1977**, *49*, 1348.

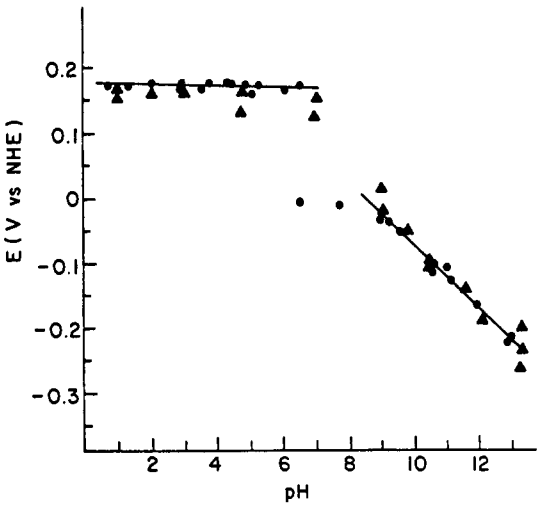

Figure 1. Potential vs. pH for the reduction of O_2 with $Fe^{II}TMPyP$ acting as catalyst: (●) $^1/_2(E_{pc} + E_{pa})$ for the reduction of $Fe^{III}TMPyP$, oxygen-free, same as the data in Figure 1 of ref 15; (▲) $E_{p,cat}$ for the reduction of O_2 via $Fe^{II}TMPyP$. The scan rate was 0.1 V/s for these experiments.

of the plates was fitted with two standard taper-glass joints. These fittings were used as ports for filling and used as ports for the reference and auxiliary electrodes. A Teflon spacer, cut to cell dimensions, was used to separate the quartz plates. The assembly was made rigid and airtight with epoxy. The path length of the OTTLE was determined by measuring the 418-nm absorbance maximum (ϵ_{418} = 1020 M^{-1} cm^{-1}) of a known concentration of $K_3Fe(CN)_6$ in nitrogen-saturated 0.1 M KCl solutions.[31] Typical cell volume was 50 μL, and the cell path length was ca. 0.05 cm.

Rotating ring-disk electrochemical (RRDE) experiments were performed with a Pine Instrument Co. Model RDE-3 potentiostat and a Model ASR-165 analytical rotator. Electrodes, purchased from the Pine Instrument Co., consisted of a platinum ring and either a glassy-carbon or a platinum disk. The dimensions of the disk, the ring, and the gap between them were determined with the use of a traveling microscope.

A Nova 3-S minicomputer (Data General Corp., Maynard, MA) was used for data acquisition, plotting, and simulation. The minicomputer was equipped with four independent, 12-bit digital-to-analog converters (DAC), a 12-bit analog-to-digital converter (ADC), and a 32-bit pulse counter. When the time frame of the experiment was sufficiently long, the pulse counter and a voltage-to-frequency converter were used for the analog-to-digital data conversion. Two of the DAC's were connected to a Houston 2000 X-Y plotter for data plotting.

Results

1. Potential Dependence of Catalysis. At scan rates of less than 0.1 V/s, the CV i–E curves exhibited reversible characteristics with the peak cathodic current, i_{pc}, equal in magnitude to the peak anodic current, i_{pa}, in thoroughly deoxygenated solutions of $Fe^{III}TMPyP$ in 0.05 M H_2SO_4. The $E_{0.85}$ of +0.18 V was identical with that determined by taking the average of the anodic and cathodic peak potentials. Upon addition of a small amount of oxygen, i_{pc} increased while i_{pa} decreased. If the $Fe^{III}TMPyP$ concentration was made equivalent to that of oxygen for an air-saturated solution, 2.4 × 10^{-4} M, i_{pc} increased by a factor of ca. 8.5 times from that of an oxygen-free solution, and i_{pa} was absent and identical with that of background without the iron porphyrin (e.g., Figure 1 of ref 1).

A plot of the CV cathodic peak potential, E_{pc}, as a function of pH for $Fe^{III}TMPyP$ in oxygen-free solutions was characterized by two regions: The first was at pH 1–6, where E_{pc} remained constant at +0.15 V and independent of pH. The second was between pH 7 and 13, where E_{pc} shifted toward negative potentials with increasing pH at a rate of ca. 60 mV/pH unit.

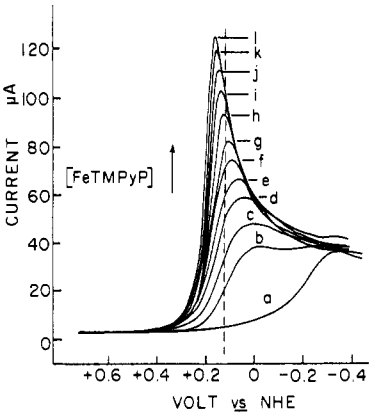

Figure 2. Cyclic voltammograms for the reduction of O_2 (0.2 mM) in 0.05 M H_2SO_4 containing various concentrations of $Fe^{III}TMPyP$ (in mM): (a) 0.0; (b) 0.022; (c) 0.044; (d) 0.085; (e) 0.13; (f) 0.20; (g) 0.25; (h) 0.37; (i) 0.51; (j) 0.63; (k) 0.83; (l) 0.99. The dashed line represents the E_{pc} value of an oxygen-free solution. The scan rate was 0.05 V/s.

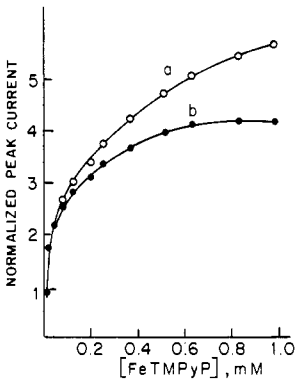

Figure 3. Plot of the normalized peak current (a) and the corrected normalized current (b) vs. $Fe^{III}TMPyP$ concentration (O_2 concentration 0.24 mM; scan rate 0.05 V/s). $i_{p,n=1}$ was calculated for the one-electron reduction of O_2 by using the Randles–Sevcik equation.

The peak potential of the catalytic i–E wave, $E_{p,cat}$, for solutions containing equimolar concentrations of oxygen and $Fe^{III}TMPyP$ was essentially identical with that obtained for the oxygen-free solutions. The pH dependence of $E_{p,cat}$ is compared to that of E_{pc} in Figure 1. As seen in this figure, these potentials virtually coincide over the pH range of 1–13. This coincidence indicates that the potential of O_2 catalysis is related closely to the redox potential of the $Fe^{III/II}TMPyP$ couple, i.e., reaction 1.

2. Concentration Dependence of Catalysis. In Figure 2, the CV i–E curves are shown for air-saturated solutions with varying amounts of $Fe^{III}TMPyP$. Curve a in this figure represents the i–E curve for oxygen in the absence of FeTMPyP. As the iron porphyrin concentration is increased from 0.02 to 0.99 mM, $E_{p,cat}$ moves toward more positive potentials. At a catalyst to oxygen concentration ratio of 4:1, $E_{p,cat}$ occurs 40 mV more positive than the E_{pc} value of $Fe^{III}TMPyP$ in oxygen-free solutions (dotted line in Figure 2). Saveant et al.[32] and Anson[33] have suggested that $E_{p,cat}$ could occur positive of the redox potential of the catalyst when the kinetic rates of

(29) Heineman, W. R.; Kuwana, T. *Acc. Chem. Res.* **1976**, *9*, 241.
(30) Murray, R. W.; Heineman, W. R.; O'Dom, G. W. *Anal. Chem.* **1967**, *39*, 1667.
(31) Angelis, T. P.; Heineman, W. R. *J. Chem. Educ.* **1976**, *53*, 594.
(32) Andrieux, C. P.; Blocman, C.; Bouchiat-Dumas, J. M.; M'Halla, F.; Saveant, J. M. *J. Electroanal. Chem. Interfacial Electrochem.* **1980**, *113*, 19.
(33) Anson, F. C. *J. Phys. Chem.* **1980**, *84*, 3336.

the E and C steps are very fast. The experimentally observed shift in $E_{p,cat}$ with the iron porphyrin concentration is in agreement with our computer-simulated potential values for an EC mechanism when the rate constant[15] of the E step is ca. 6×10^{-3} cm/s and the rate constant[34] of the C step is greater than ca. 5×10^6 M^{-1} s^{-1}.

In Figure 3, a normalized peak current function, $i_{p,N}$, is plotted vs. the FeTMPyP concentration for oxygen catalysis. The normalization involves the $i_{p,cat}$ value taken from Figure 2 being divided by the peak current, $i_{p,n=1}$, that would have resulted if oxygen were reduced by an one-electron process to superoxide ion. The $i_{p,n=1}$ value is calculated from the Randles-Sevcik equation[35]

$$i_{p,n=1} = (2.67 \times 10^5)n^{3/2}AC_0D_0^{1/2}v^{1/2} \quad (3)$$

where the bulk concentration of oxygen, C_0, was 0.24 mM, the diffusion coefficient of oxygen,[36] D_0, was 2.0×10^{-5} cm^2/s, the electrode area, A, was 0.39 cm^2; the scan rate, v, was 0.05 V/s, and $n = 1$ for O_2 reduction to superoxide. This equation is valid for a reversible, diffusion-controlled electrode reaction. As can be seen from Figure 3, $i_{p,N}$ increases rapidly with the FeTMPyP concentration up to a concentration of ca. 5×10^{-4} M. No reverse anodic current is observed on the reverse CV scan until this concentration is attained. Curve b of Figure 3 is the corrected normalized current, $i_{p,N,cor}$, which is calculated by subtracting from $i_{p,cat}$ the peak current contributed by the reduction of $Fe^{III}TMPyP$ to $Fe^{II}TMPyP$ as determined from the reduction of the iron porphyrin in oxygen-free solutions. The $i_{p,cat,cor}$ plot yields a limiting value of 4.1, suggesting that oxygen is being reduced to water when the FeTMPyP to oxygen concentration ratio becomes greater than ca. 2:1.

At a porphyrin concentration of 2.5×10^{-4} M in an air-saturated solution (i.e., concentration ratio of 1:1), an $i_{p,cat}$ of 78 μA was observed experimentally (see curve g, Figure 2). If this peak current is analyzed with the assumption of the validity of eq 3, an n value of 2.2 can be calculated by using the concentration and diffusion coefficient of oxygen and was previously[1] interpreted as indicative of oxygen being reduced to hydrogen peroxide. On the other hand, if one computes an $i_{p,N,cor}$ value for the 1:1 concentration ratio, one would conclude that n is on the order of 3.1, as may be seen from the plot of $i_{p,N,cor}$ in Figure 3.

The magnitude of $i_{p,cat}$ depends on the extent of the overlap between the wave for O_2 catalysis and that of the mediator. Computer simulation of the EC mechanism indicates that the $i_{p,cat}$ is given by[34]

$$i_{p,cat} = (2.67 \times 10^5)N_1(1.09)AC_0D_0^{1/2}v^{1/2} + i_{p,M} \quad (4)$$

where N_1 is a linear multiplier reflecting the stoichiometry of the C reaction (replacing the usual n of eq 3), and $i_{p,M}$ is the peak current due to the mediator/catalyst (i.e., iron porphyrin in the present case). The $i_{p,cat}$ value maximizes when the conditions are such that the catalytic wave coincides with and is "stacked" onto the mediator/catalyst wave. If the potential of the catalytic wave shifts in either a positive or a negative direction, the two waves will deconvolute and the peak current will decrease. Thus, caution must be exercised in interpreting the magnitude of the $i_{p,cat}$ value in terms of the parameters governing the EC mechanism. Nonetheless, it is clear from data in Figure 3 that oxygen can be reduced catalytically by the iron porphyrin and that the extent of reduction depends on the concentration ratios of porphyrin to oxygen.

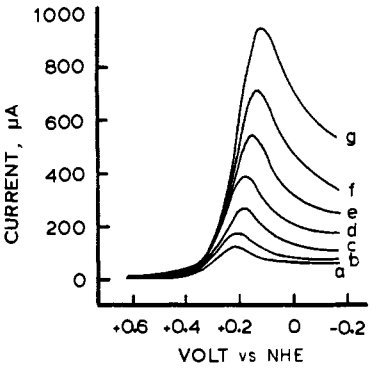

Figure 4. Cyclic voltammograms for the reduction of 2.4×10^{-5} M O_2 by 5.3×10^{-4} M $Fe^{III}TMPyP$ in 0.05 M H_2SO_4 at various scan rates (in V/s): (a) 0.005; (b) 0.010; (c) 0.025; (d) 0.050; (e) 0.100; (f) 0.200; (g) 0.400.

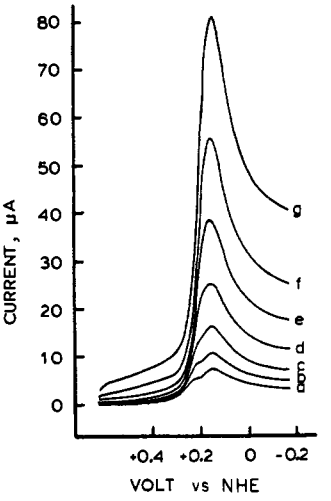

Figure 5. Cyclic voltammograms for the catalytic reduction of 1.3×10^{-3} M O_2 by 5.3×10^{-4} M $Fe^{III}TMPyP$ in 0.05 M H_2SO_4 at various scan rates (in V/s): (a) 0.005; (b) 0.010; (c) 0.025; (d) 0.050; (e) 0.100; (f) 0.200; (g) 0.400.

3. Scan Rate Dependence. The i–E curves for the catalytic reduction of O_2 at various scan rates (5–0.40 V/s) are shown in Figures 4 and 5. The concentration of $Fe^{III}TMPyP$ was 5.3×10^{-4} M in 0.05 M H_2SO_4 while the concentrations of O_2 were 2.4×10^{-5} and 1.3×10^{-3} M in the data of Figures 4 and 5, respectively. Thus, the porphyrin to oxygen concentration ratios were 22:1 and 0.4:1.

A unique feature of these i–E waves at the lower scan rates as seen in Figure 4 is the appearance of a double wave, which is due to the depletion of O_2 in the reaction layer next to the electrode surface prior to the depletion of the $Fe^{III}TMPyP$. The two factors that are germane to the double wave are the large iron porphyrin to O_2 concentration ratio and the slow scan rate.

The catalytic i–E wave shifts to more negative potentials with increasing scan rate, eventually convoluting with the wave due to the reduction of $Fe^{III}TMPyP$ at high scan rates. For example, at a scan rate of 0.4 V/s, the $E_{p,cat}$ is +0.156 V compared to a value of +0.151 for the catalyst in the absence of oxygen.

At a $Fe^{III}TMPyP$ to O_2 concentration ratio of 0.4:1, the i–E curve does not appear as a double wave at a scan rate of 5 mV/s because the relatively large O_2 concentration could not be depleted in the diffusion layer before the E_{pc} of the $Fe^{III/II}TMPyP$ couple was reached (see curve a, Figure 5).

(34) DiMarco, D. M.; Forshey, P. A.; Kuwana, T. "Chemical Modification of Surfaces"; Miller, J., Ed.; American Chemical Society: Washington, DC, 1982; ACS Symp. Ser. No. 192, pp 72–97.
(35) Bard, A. J.; Faulkner, L. R. "Electrochemical Methods, Fundamentals and Applications"; Wiley: New York, 1980; p 675.
(36) The value of 2.0×10^{-5} cm^2/s used for the calculation was an average of 1.67×10^{-5} cm^2/s (from ref 17) and 2.5×10^{-5} cm^2/s (Kolthoff, I. M.; Miller, C. S. *J. Am. Chem. Soc.* **1941**, *63*, 1013).
(37) Kobayashi, N.; Fujihira, M.; Osa, T.; Kuwana, T. *Bull. Chem. Soc. Jpn.* **1980**, *53*, 2195–2200.

Table I. Comparison of $i_{p,cat}$ in Acidic and Basic Solutions[a]

scan rate, V/s	$i_{p,cat}$(pH 1.5), μA	$i_{p,cat}$(pH 10.1), μA	i_p(pH 10.1)/ i_p(pH 1.5)
0.005	114	114	1.00
0.010	163	164	1.01
0.025	255	238	0.93
0.050	375	343	0.93
0.100	515	454	0.88
0.200	683	598	0.88
0.400	889	796	0.89

[a] The solution conditions were 5.3×10^{-4} M FeTMPyP, 1.3×10^{-3} M oxygen, and 0.05 M H_2SO_4 for pH 1.5 and 0.1 M $NaHCO_3$ and NaOH adjusted to pH 10.1.

The $i_{p,cat}$ was plotted as a function of the square root of scan rate for 5.2×10^{-4} M $Fe^{III}TMPyP$ in 0.05 M H_2SO_4 while the oxygen concentrations were varied from 2.7×10^{-5} to 1.3×10^{-3} M. These plots were nonlinear due to the extent of overlap between the oxygen catalysis current and the i–E wave of the iron porphyrin. The resultant i–E waves are illustrated in Figure 4 and are a convolution of these two components. However, the important feature of these plots was the calculated $i_{p,N,cor}$ values. At low scan rates and the higher iron porphyrin to oxygen concentrations, $i_{p,N,cor}$ was calculated to be ca. 4, whereas at high scan rates and lower concentration ratios, the calculated value approached 2. The data suggest again that the mechanism of O_2 reduction by iron porphyrin involves a series pathway with hydrogen peroxide as a possible initial product.

The $i_{p,cat}$ was evaluated as a function of pH from values of 1 to 13. A monomer–dimer equilibrium exists[15,20,21] in alkaline solutions so that the $Fe^{III}TMPyP$ concentration (monomer) is lowered considerably. For example, ca. 48% of a 5.2×10^{-4} M iron porphyrin solution exists as a monomer at pH 10.1 (0.1 M $NaHCO_3$). Nevertheless, the CV catalytic i–E waves are very similar to those in acidic solutions when one corrects to the monomer concentration. At slow scan rates there is sufficient time for the dimer to dissociate to the monomer during the CV scan time; hence, the $i_{p,cat}$ value approaches that accountable by the total analytical concentration of iron porphyrin in the solution. The $i_{p,cat}$ vs. scan rate for the reduction of oxygen in acidic and basic solutions, 0.05 M H_2SO_4 and 0.1 M $NaHCO_3$, is compared in Table I. The decrease in the ratio of $i_{p,cat}$ with increasing scan rate reflects the extent of dimer dissociation during the time span of the CV scan. It is interesting to note that, if one conducts a fast CV scan, for example, at 0.2 V/s, in alkaline solutions when the iron porphyrin to oxygen ratio is relatively small, two $i_{p,cat}$ waves are observed. The first one is the usual catalytic wave due to the reduction of the monomer. The second wave at more negative potentials corresponds to the reduction of the dimer, which, upon reduction, readily dissociates[15] to the monomer $Fe^{II}TMPyP$, which is our "active" catalyst.

4. Thin-Layer-Cell Coulometry. The stoichiometry of the O_2 catalysis by FeTMPyP was evaluated by conducting CV experiments in a thin-layer cell with either a Au minigrid or a glassy-carbon electrode. In these experiments the electrode potential was slowly scanned from a +0.38 to −0.02 V. The scan rate was sufficiently slow to insure the quantitative reduction of all electroactive species within the potential width. The areas under the resulting i–E curves were used to calculate the charge and hence, the extent of O_2 reduction.

A typical thin-layer i–E curve is shown in Figure 6 for the reduction of $Fe^{III}TMPyP$ containing O_2. On the initial cathodic scan, the charge, Q, corresponds to the four-electron reduction of O_2 and the one-electron reduction of $Fe^{III}TMPyP$. During all subsequent scans (e.g. curve b, Figure 6), the cathodic and anodic charges were equal and accounted for by the $Fe^{III}TMPyP$ reduction. Thus, the i–E curves for the second

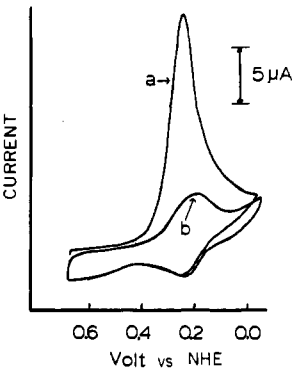

Figure 6. Cyclic voltammogram for the thin-layer-cell reduction of 2.4 mM O_2 and 2.0 mM $Fe^{III}TMPyP$ in 0.05 M H_2SO_4 (cell volume 8.7×10^{-6} L; scan rate 0.0024 V/s): (a) first cathodic scan; (b) second cathodic scan after O_2 depletion.

Table II. Thin-Layer Coulometric Data

$[O_2]$, mM	$[Fe^{II}TMPyP]$, mM	n[a]
0.24	0.21 (pH 1.5)	4.06
0.24	0.30 (pH 2.5)	3.99
0.24	0.20 (pH 5)	3.85
1.32	0.31 (pH 7)	4.01
0.24	0.30 (pH 11)	4.02
		av 3.99 (±0.08)
0.8 (H_2O_2)	0.31 (pH 7)	1.93 (±0.10)

[a] The charge used to calculate these n values was corrected for the charge due to $Fe^{III}TMPyP$ reduction.

Table III. Kinetic Rate of H_2O_2 Disproportionation by $Fe^{III}TMPyP$

k, M^{-1} s^{-1}	pH	soln conditions
17 (±2)	1.5	0.05 M H_2SO_4
5 (±2)	5.6	0.10 M NaH_2PO_4 + 0.004 M NaOH
39 (±4)	7.0	0.05 M NaH_2PO_4 + 0.05 M Na_2HPO_4
$1.3 (\pm 0.4) \times 10^3$	9.1	0.05 M $Na_2B_4O_7$
$1.1 (\pm 0.3) \times 10^4$	13	0.10 M NaOH

and all subsequent scans indicated that O_2 had been depleted in the confines of the thin-layer cell. The results of these thin-layer coulometry experiments for various pH conditions are summarized in Table II. The average value of n equal to 3.99 (±0.08) supports the conclusions that O_2 can be quantitatively reduced to water by electrogenerated $Fe^{II}TMPyP$.

5. Disproportionation of Hydrogen Peroxide. The kinetic rate for the disproportionation of H_2O_2 with $Fe^{III}TMPyP$ acting as a catalyst was determined by monitoring the concentration of H_2O_2 at a Au or Pt microelectrode as a function of time. The electrode potential required to oxidize H_2O_2 was pH dependent, ranging from +1.2 V at pH 1.5 to +0.3 V at pH 13. The H_2O_2 concentration was determined from the oxidative current by comparison with a predetermined calibration curve. Experimentally, $Fe^{III}TMPyP$ was injected into a rapidly stirred H_2O_2 solution, and the decay current was recorded. The solution pH was controlled by appropriate buffer solutions (see Table III), while the $Fe^{III}TMPyP$ stock solution was unbuffered and slightly acidic to prevent dimerization.

The plots of the logarithm of the H_2O_2 concentration, normalized to that concentration at $t = 0$, vs. time at pH 7.0 were linear as seen in Figure 7. The slopes of these plots were linearly dependent on the $Fe^{III}TMPyP$ concentration. The iron porphyrin and H_2O_2 dependence indicated that the rate-limiting step for the disproportionation was first order in both hydrogen peroxide and iron porphyrin. Similar experiments were conducted at pHs ranging from 1.5 to 13. The rate constants for the disproportionation increased from ca. 17 to

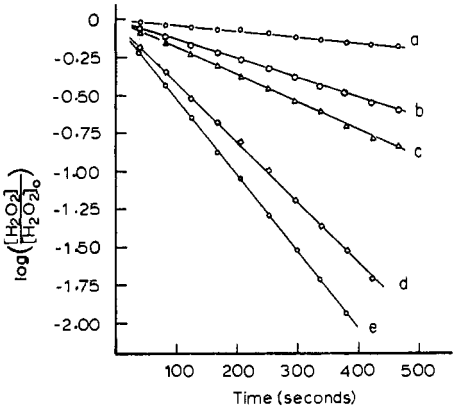

Figure 7. Plot of the logarithm of the normalized concentration of H_2O_2 vs. time for the oxidation of H_2O_2 at a gold electrode in pH 7 phosphate buffer. The solutions were swiftly stirred, and at t = 0, various concentrations of $Fe^{III}TMPyP$ were injected (in mM): (a) 0.22; (b) 0.83; (c) 0.87; (d) 2.1; (e) 2.7.

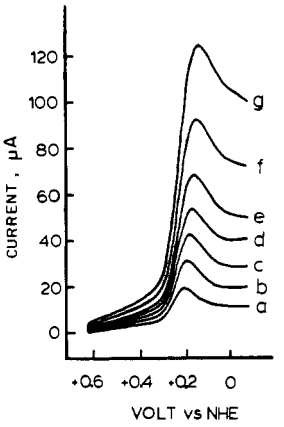

Figure 8. Cyclic voltammograms for the reduction of H_2O_2 catalyzed by $Fe^{II}TMPyP$ in oxygen-free 0.05 M H_2SO_4: H_2O_2 concentrations (in mM) (a) 0.31, (b) 0.24, (c) 0.19, (d) 0.15, (e) 0.12, (f) 0.10, (g) 0.076; scan rates (in V/s) (a) 0.167, (b) 0.125, (c) 0.083, (d) 0.067, (e) 0.050, (f) 0.030, (g) 0.017. The $Fe^{III}TMPyP$ concentration was 0.13 mM.

1.1×10^4 M^{-1} s^{-1} at pH values of 1.5 and 13, respectively. The results are summarized in Table III. The largest rate constant measured at pH 13 is still ca. 3 orders of magnitude less than the value of 10^7 M^{-1} s^{-1} reported for the disproportionation of H_2O_2 by the catalase enzyme system.[38]

6. Decomposition of the Ferric Porphyrin by H_2O_2. Pasternack et al.[39] reported that $Fe^{III}TMPyP$ underwent an irreversible modification (thought to be oxidation of the porphyrin ring) during a superoxide dismutase reaction with the superoxide ion. Hydrogen peroxide, a product of the dismutase reaction, was reported as being responsible for this decomposition. Superoxide ions and hydroxy radicals (·OH) were shown to be unreactive with respect to porphyrin decomposition. Since any $Fe^{III}TMPyP$ decomposition would limit the use of this porphyrin as a catalyst, the rate of decomposition of $Fe^{III}TMPyP$ by H_2O_2 was quantitated, with use of the stopped-flow technique.

The $Fe^{III}TMPyP$ concentration in 0.05 M H_2SO_4 was monitored by following the 400-nm absorbance maximum of the ferric porphyrin. Pseudo-first-order conditions were maintained by a 100-fold excess of H_2O_2. Plots of ln [$Fe^{III}TMPyP$] vs. time were linear over a 6-fold time interval and the reaction was found to fit the rate law

$$d[Fe^{III}TMPyP]/dt = k[Fe^{III}TMPyP][H_2O_2] \quad (5)$$

The rate constant, k, for this reaction was calculated to be 5.3 (±0.4) M^{-1} s^{-1} in 0.05 M H_2SO_4 and 10.1 (±0.5) M^{-1} s^{-1} in 0.1 M phthalate buffer, pH 4.0. The rate of this reaction was not determined at higher pH values since the rate of the disproportionation reaction became appreciable so that pseudo-first-order conditions could no longer be maintained. The result of a thin-layer reduction of hydrogen peroxide in an oxygen-free solution of $Fe^{III}TMPyP$ is included in Table II. The n value of 1.9 calculated from the charge with the known concentration of hydrogen peroxide indicates that it is quantitatively reduced to water. Because there was a question of the Au minigrid catalyzing hydrogen peroxide decomposition, the oxygen and hydrogen peroxide reductions were repeated with a glassy-carbon electrode. The results were identical within experimental error.

Finally, optically coupled thin-layer cell (OTTLE) experiments with a Au minigrid provided a convenient way to evaluate the extent of FeTMPyP decomposition by oxygen. For example, the OTTLE cell was filled with an air-saturated solution with 2.5×10^{-4} M $Fe^{III}TMPyP$ (iron porphyrin to oxygen ratio ca. 1:1) in 0.05 M H_2SO_4. The optical absorbance at 400 nm was monitored prior to, and during, exhaustive reduction at −0.25 V and after the system was open-circuited and oxygen was allowed to diffuse into the cell to reoxidize $Fe^{II}TMPyP$. For this solution, one complete redox cycle resulted in a decrease of the 400-nm absorbance by less than 1%.

7. Hydrogen Peroxide Reduction by Ferrous Porphyrin. Since the disproportionation of hydrogen peroxide by $Fe^{III}TMPyP$ was found to be slow in 0.05 M H_2SO_4, solutions of $Fe^{III}TMPyP$ containing H_2O_2 could be prepared with relatively low concentrations of O_2. As discussed previously, thin-layer coulometry experiments indicated that H_2O_2 could be quantitatively reduced by electrogenerated $Fe^{II}TMPyP$ with a stoichiometry of 2.

CV i–E curves for the reduction of H_2O_2 are reproduced in Figure 8. Between each of the CV scans, the solution was purged by nitrogen to ensure the removal of any O_2. Because there was finite change in the H_2O_2 concentration during successive CV scans, the H_2O_2 concentration was assessed between scans by monitoring the current at a rotating Pt-ring electrode that was potentiostated at +1.2 V. The plots of $i_{p,cat}$ vs. the square root of the scan rate were linear when normalized to the experimentally determined H_2O_2 concentrations. Thus, plots of such adjusted $i_{p,cat}$ vs. $v^{1/2}$ were linear over the scan rates of 0.017–0.17 V/s. The stoichiometric ratio (see eq 4) of these plots gave a value of 2.1 (±0.2), which is indicative of a two-electron reduction of H_2O_2. A diffusion coefficient[40] of 6.8×10^{-6} cm^2/s and the experimentally determined H_2O_2 concentrations were used in the calculations.

8. Computer Simulations. The CV i–E profiles for the O_2 catalysis by iron porphyrin were simulated with use of the finite difference method.[41] The computer programs were designed to account for the kinetic rates of both the heterogeneous electron-transfer rate, k_s, of reaction 1′ and the homogeneous reactions, k_f, the differences in the diffusion coefficients of the reactants, the concentrations of the electroactive and other species in the reaction sequence, and the stoichiometry (N) of any homogeneous reactions. The E-step reaction was assumed to follow the Butler–Volmer requirements.[42] Three

(38) Boyer, P. D.; Lardy, H.; Myrbaeck, K. *Enzymes, 2nd ed.* **1963**, *8*, 257.
(39) Pasternack, R. F.; Halliwell, B. *J. Am. Chem. Soc.* **1979**, *101*, 1026.
(40) Littauer, E. L.; Tsai, K. C. *Electrochim. Acta* **1979**, *24*, 351.
(41) (a) Ruzic, J.; Feldberg, S. W. *J. Electroanal. Chem. Interfacial Electrochem.* **1974**, *50*, 153–162. (b) Feldberg, S. W. In "Electroanalytical Chemistry"; Bard, A. J., Ed.; Marcel Dekker: New York, 1969; Vol. 3, pp 199–296.
(42) (a) Butler, J. A. V. *Trans. Faraday Soc.* **1924**, *19*, 729. (b) Volmer, M.; Erdy-Gruz, T. *Z. Phys. Chem., Abt. A* **1930**, *150*, 203.

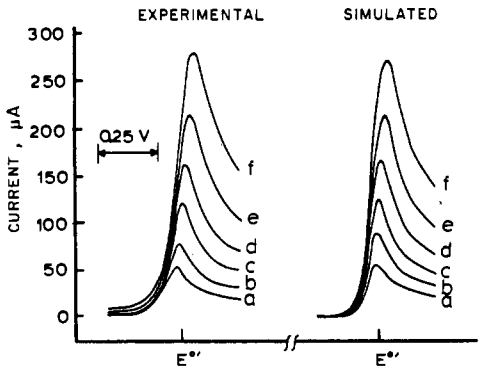

Figure 9. Experimental and simulated cyclic voltammetric curves for the reduction of O_2 by $Fe^{II}TMPyP$ ($[O_2]$ = 2.4 mM; $[Fe^{III}TMPyP]$ = 5.3 mM) at the following scan rates (in V/s): (a) 0.010; (b) 0.025; (c) 0.050; (d) 0.100; (e) 0.200; (f) 0.400.

different EC catalytic mechanisms for oxygen catalyzed by $Fe^{II}TMPyP$ were considered:[34]

(I) E step

$$Fe^{III}TMPyP + e^- \xrightarrow{k_s} Fe^{II}TMPyP \qquad (1')$$

and C step

$$2Fe^{II}TMPyP + O_2 + 2H^+ \xrightarrow{k_{f1}} 2Fe^{III}(TMPyP) + H_2O_2 \qquad (6)$$

(II) reaction 1′ followed by

$$4Fe^{II}TMPyP + O_2 + 4H^+ \xrightarrow{k_{f1}'} 4Fe^{III}TMPyP + 2H_2O \qquad (7)$$

and (III) reactions 1′ and 6 followed by

$$2Fe^{II}TMPyP + H_2O_2 + 2H^+ \xrightarrow{k_{f2}} 2Fe^{III}TMPyP + 2H_2O \qquad (8)$$

where reactions 6–8 reflected the reactant stoichiometry in the homogeneous steps. In these simulated mechanisms, it was assumed that a single bimolecular reaction was rate limiting, irrespective of the stoichiometry. Additional information concerning the use and verification of the simulation programs can be found in the discussion by DiMarco et al.[34]

The *i–E* profiles simulated for mechanisms I and II could not account for the experimental results over a wide variation of scan rate and concentration ratios of iron porphyrin to oxygen. The best fit between experimental and simulated *i–E* profiles was obtained consistently with the modeling of mechanism III, henceforth referred to as the "2 + 2" mechanism (i.e., $N_1 = 2$, $N_2 = 2$). The results of simulating this mechanism are summarized in Table IV, and the *i–E* profiles are shown in Figure 9. As may be seen in this figure, the shapes of the experimental and simulated *i–E* profiles are nearly identical over a wide range of scan rates for the concentration ratio used. The data in Table IV indicate that the peak potentials agreed within 4 mV and the peak currents within 4% between the simulated and experimental results.

Since the heterogeneous rate constant, k_s, varies depending on the state of the electrode surface at the time of the experiment, the value of k_s used in the simulations was that determined experimentally (k_s = 0.024 cm/s) for FeTMPyP in oxygen-free solutions at a highly polished glassy-carbon electrode. The electrode and solution conditions, except for the absence of O_2, were identical with those for the experimental *i–E* curves in Figure 9. For comparison, starting and final potentials, scan rates, etc. used in the simulations were identical with those evaluated experimentally. The value of k_{f1} was that determined by rotating ring-disk electrode

Table IV. Comparison of Simulated and Experimental Cyclic Voltammetric Curves[a]

scan rate, V/s	i_p^S, μA	i_p^E, μA	i_p^S/i_p^E	$E_p^S - E^{o'}$, mV	$E_p^E - E^{o'}$, mV	ΔE_p, mV
	$[O_2] = 2.4 \times 10^{-4}$ M; $[Fe^{III}TMPyP] = 5.3 \times 10^{-4}$ M					
0.010	52.5	50.5	1.04	+10	+20	10
0.025	84.8	76.0	1.11	+2	+8	6
0.050	119.4	118	1.01	−8	−6	2
0.100	160.4	160	1.01	−20	−20	0
0.200	208.7	206	1.01	−20	−20	0
0.400	264.6	265	1.00	−44	−50	6
	$[O_2] = 2.4 \times 10^{-5}$ M					
0.005[b]	5.1	4.9	1.04	+58	+50	8
0.005[b]	7.5	6.8	1.10	−26	−25	1
0.010[b]	7.6	7.7	0.99	+45	+42	3
0.010[b]	10.6	10.1	1.05	−24	−25	1
0.050	24.2	23.0	1.05	−24	−21	3
0.100	35.0	34.6	1.01	−22	−20	2
			av 1.04 (±0.04)		av	4 (±3)

[a] The superscript E represents experimental data; the superscript S represents simulated data. [b] Under these conditions the double-wave phenomenon was observed; the i_p^E values of 4.9 and 7.7 μA correspond to the peak current of the first wave while those at 6.8 and 10.1 μA correspond to the peak current of the second wave.

(RRDE) experiments for the oxidation of $Fe^{II}TMPyP$ by oxygen ($k_{f1} = 1.5 \times 10^7$ M^{-1} s^{-1}). The details of the RRDE work will be published elsewhere.[43] The value of the second homogeneous rate constant, k_{f2}, was varied until the peak currents of the simulated curves matched those of the experimental ones. A value of 2.5×10^5 M^{-1} s^{-1} for k_{f2} was found to be appropriate for the simulations over a wide range of scan rates and concentration ratios.

The effects of changing k_s, k_{f1}, or k_{f2} were studied to determine the range of these parameters that would still yield acceptable results. Changing k_s by one order of magnitude in either direction affected primarily the value of $E_{p,cat}$ and not significantly the $i_{p,cat}$. Decreasing k_{f1} to 1.0×10^7 M^{-1} s^{-1} resulted in shifting $E_{p,cat}$ negatively by 8 mV at a scan rate of 0.1 V/s. Decreasing k_{f2} to 2.0×10^5 M^{-1} s^{-1} gave a 4-μA decrease in $i_{p,cat}$ and a 1-mV shift in $E_{p,cat}$. Increasing the rates by the same amount resulted in corresponding opposite shifts. Since shifts of 1–2 mV in $E_{p,cat}$ and 1–2 μA in $i_{p,cat}$ could be easily observed experimentally, the agreement between the simulated and experimental results gave credence to the values of the kinetic rates within an estimated error of ±10%. Although other combinations of simulator parameters and mechanisms could possibly produce similar *i–E* profiles, it was felt that the use of experimentally determined parameters in the simulation lent confidence to the results.

Discussion and Conclusions

The CV and thin-layer coulometric results support the conclusion that oxygen is reduced to water rapidly via the electrogenerated ferrous porphyrin. A most likely mechanism appears to be through the initial formation of hydrogen peroxide, which then undergoes a "direct" reduction by ferrous porphyrin. The computer-simulated CV *i–E* profiles were in good agreement with the experimental ones for a mechanism involving oxygen reduction through hydrogen peroxide in a series pathway, the "2 + 2 mechanism".

The question is as follows: "How does $Fe^{II}TMPyP$ reduce oxygen to hydrogen peroxide or hydrogen peroxide to water when these products each require two electrons?" Thermodynamically, the one-electron reduction of O_2 to superoxide ion by $Fe^{II}TMPyP$, on the basis of redox potentials, is unfa-

(43) Forshey, P. A.; Kuwana, T., manuscript in preparation. Forshey, P. A. Ph.D. Thesis, The Ohio State University, 1982.

vorable by 0.5 V.[15,44] This was pointed out by Pasternack and Halliwell[39] in their study of the superoxide dismutase activity of $Fe^{II}TMPyP$. In their report, superoxide was removed by $Fe^{III}TMPyP$ at a rate of 3×10^7 M^{-1} s^{-1} at pH 10. The suggested mechanism involved the reduction of $Fe^{III}TMPyP$ by superoxide to $Fe^{II}TMPyP$ followed by the reduction of superoxide to hydrogen peroxide by $Fe^{II}TMPyP$. Although we believe that this latter reaction is unlikely, it is interesting to note that the rate constant of 3×10^7 M^{-1} s^{-1} for the reaction between $Fe^{III}TMPyP$ and superoxide is similar in magnitude to that of 1.5×10^7 M^{-1} s^{-1} for the removal of $Fe^{II}TMPyP$ by O_2 as determined by RRDE experiments.[43]

A suggested mechanistic pathway that would alleviate such an apparent discrepancy is to suggest that these reactions proceed via a common intermediate such as an iron porphyrin–oxygen complex. An intermediate such as this has been proposed[45] for the reaction of iron hemes with O_2 and confirmed recently with use of iron tetraphenylporphyrin at low temperatures in nonaqueous solvents.[46] A reaction consistent with the above observations would involve reaction 1 followed by

$$Fe^{II}TMPyP + O_2 + = Fe^{III}TMPyP\text{–}O_2^- \quad (9)$$

$$Fe^{III}TMPyP\text{–}O_2^- + 2H^+ + Fe^{II}TMPyP = 2Fe^{III}TMPyP + H_2O_2 \quad (10)$$

where the intermediate is further reduced by $Fe^{II}TMPyP$ or an electron from the electrode. The formalism used to denote the intermediate suggests electron transfer from the iron porphyrin to the oxygen. However, the extent of charge transferred for intermediates of this type may range from the experimentally determined value of ca. 80%[47] to a theoretical value of near zero.[48] For reaction 10 to occur, the redox potential of the intermediate must be equivalent to, or more positive in value than, the redox potential of the $Fe^{III/II}TMPyP$ couple.

The proposed reaction scheme is further supported by the pulse radiolysis results of Farragi and Bettelheim,[49] who found that the rate of the $Fe^{II}TMPyP$ and O_2 reaction was first order in O_2 and second order in $Fe^{II}TMPyP$. They suggested the same intermediate as written in reactions 9 and 10. Their studies also indicated that no reaction occurred when the axial position of the iron porphyrin was blocked by ligands such as cyanide ion. It may be significant to note that an axial position is available for reaction with O_2 in the postulated five-coordinate ferrous $Fe^{II}TMPyP$, as supported by magnetic circular dichroism measurements.[50] The availability of this position would offer a minimal barrier to interaction with O_2.

A reaction pathway allowing a two-electron reduction of hydrogen peroxide to water may involve an intermediate complex similar to that of oxygen with the iron porphyrin. Such complexes have been suggested as intermediates in the reaction of peroxidase enzymes with hydrogen peroxide.[51] Similar to the case for the porphyrin–oxygen complex, a porphyrin–hydrogen peroxide intermediate could be reduced by another ferrous porphyrin or by the electrode.

The proposed "2 + 2" mechanism is consistent with several reports in the literature. For example, Kolpin and Swofford[12] have shown that hemes adsorbed on a mercury electrode could reduce oxygen to water. They suggested that the complexes of Fe^{II} heme–O_2 and Fe^{II} heme–H_2O_2 were involved in the rate-limiting steps of the overall reduction process. Collman et al.[11,16] have reported that an intermediate in the reduction of oxygen with their cofacial porphyrin was a μ-peroxo species. Yeager et al.,[17] Kozawa et al.,[6] and Van Veen et al.[52] have apparently detected various amounts of H_2O_2 in their studies of O_2 reduction by adsorbed metal phthalocyanines. The amount of H_2O_2 seemed to depend on the reaction conditions and the pretreatment of the catalyst and the electrode surface. Van Veen also reported that the activity of the metal phthalocyanine toward O_2 reduction was directly related to the rate of H_2O_2 decomposition by the catalyst.

The reduction of O_2 to water by a "direct" four-electron process has been suggested.[5-7,10,11,53-59] However, H_2O_2 may be an important species in all experiments concerning the reduction of oxygen by adsorbed catalysts. Whether H_2O_2 becomes an intermediate or product appears to depend on the reactivity of the catalyst toward H_2O_2. For example, we have found that CoTMPyP and CoTPyP have little reactivity to H_2O_2 and, hence, hydrogen peroxide can be electrogenerated in quantitative yield with use of these compounds as catalysts for O_2 reduction.[60]

Our rationale for the detailed examination of the homogeneous catalysis is predicated on the assumption that immobilization of the catalyst on an electrode surface will create a catalytic electrode. The mechanistic understanding provided through the homogeneous studies should assist in the usually difficult elucidation of heterogeneous catalysis. The successful immobilization of iron porphyrins on carbon electrodes and subsequent oxygen catalysis has been demonstrated by Bettelheim et al.[4] and Rocklin et al.[61] The correspondence between the electrode potential for oxygen catalysis and that of the porphyrin is supportive of an EC catalytic mechanism. Furthermore, the observation that the extent of oxygen reduction is dependent on the amount of catalyst immobilized within the polymer film on the electrode surface[4] appears to be consistent with the concentration dependence found in the present study for the homogeneous case.

A major assumption in the present work is that the amount of FeTMPyP adsorbed on the surface is nil or is negligibly small and does not affect the interpretation of the results. There are two observations that support this assumption. The first is that the agreement between the experimental and

(44) Sawyer, D. T.; Seo, E. T. *Inorg. Chem.* **1977**, *16*, 499.
(45) (a) Collman, J. P.; Gagne, R. R.; Reed, C. A.; Halbert, T. R.; Lang, G.; Robinson, W. T. *J. Am. Chem. Soc.* **1975**, *97*, 1427. (b) Basolo, F.; Hoffman, B. M.; Ibers, J. A. *Acc. Chem. Res.* **1975**, *8*, 384. (c) Drago, R. S.; Beugelsdijk, T.; Beese, J. A.; Canady, J. P. *J. Am. Chem. Soc.* **1978**, *100*, 5374. (d) Summerville, D. A.; Jones, R. D.; Hoffman, B. M.; Basolo, F. *J. Chem. Educ.* **1979**, *56*, 157.
(46) McCandlish, E. M.; Miksztal, A. R.; Nappa, M.; Spencer, A. Q.; Valentine, J. S.; Strong, J. D.; Spiro, T. G. *J. Am. Chem. Soc.* **1980**, *102*, 4268.
(47) Drago, R. S.; Corden, B. D. *Acc. Chem. Res.* **1980**, *13*, 353.
(48) Goddard, W. A., III; Olafson, B. D. "Biochemical and Clinical Aspects of Oxygen"; Caughley, W., Caughley, H., Eds.; Academic Press: New York, 1979; p 87.
(49) Farragi, M.; Bettelheim, A., private communication, Nuclear Research Center-Negev, Beer-sheva, Israel.
(50) Kobayashi, N.; Osa, T.; Hatano, M.; Kuwana, T., manuscript in preparation.
(51) Boyer, P. D.; Lardy, H.; Myrbaeck, K. *Enzymes, 2nd ed.* **1963**, *8*, 246.
(52) (a) Van Veen, J. A. R.; Visser, C. *Electrochim. Acta* **1979**, *24*, 921. (b) Van Veen, J. A. R. Ph.D. Thesis, University of Leyden, Leyden, The Netherlands, 1981.
(53) Jasinski, R. *Nature (London)* **1964**, *201*, 1212.
(54) Jahneke, H.; Schonborn, M.; Zimmerman, G. *Top. Curr. Chem.* **1976**, *61*, 133.
(55) Kozawa, A.; Zilionis, V. E.; Brodd, R. J. *J. Electrochem. Soc.* **1971**, *118*, 1705.
(56) Ulstrup, J. *J. Electroanal. Chem. Interfacial Electrochem.* **1977**, *79*, 191.
(57) Yeager, E. *J. Electrochem. Soc.* **1981**, *128*, 160C and references therein.
(58) (a) Brdicka, R.; Tropp, C. *Biochem. Z.* **1937**, *289*, 301. (b) Brdicka, R.; Weisner, K. *Naturwissenschaften* **1943**, *31*, 247. (c) Brdicka, R.; Weisner, K. *Collect. Czech. Chem. Commun.* **1947**, *12*, 39.
(59) (a) Brezina, M. *Collect. Czech. Chem. Commun.* **1957**, *22*, 339. (b) Brezina, M.; Hofmanova-Matejkova, A. *Ibid.* **1973**, *38*, 3024. (c) Brezina, M.; Khalik, W.; Koryta, J.; Musilova, M. *J. Electroanal. Chem. Interfacial Electrochem.* **1977**, *77*, 237.
(60) Chan, R. J. H.; Kuwana, T., manuscript in preparation.
(61) Rocklin, R. D.; Murray, R. W. *J. Electroanal. Chem. Interfacial Electrochem.* **1979**, *100*, 271.

simulated CV i-E profiles is excellent for an EC mechanism over a wide range of concentration ratios and scan rates. The second is that there is no evidence for O_2 catalysis with an electrode that has been exposed to a FeTMPyP solution and then thoroughly rinsed with distilled water in contrast to the case of CoTMPyP and CoTPyP, where strong surface adsorption occurs. We do recognize, however, that FeTMPyP adsorption can occur, depending on the anion present in solution. Thus, adsorption of FeTMPyP is evident when perchlorate, borate, iodide, or bromide are present in solution.

Acknowledgment. This work was supported by grants from the U.S. Air Force Office of Scientific Research and the National Science Foundation. Helpful discussions with H. Blount, D. Karweik, and D. DiMarco are hereby acknowledged. This work was also a part of the cooperative research conducted under the NSF/JSPS with Professor T. Osa and his co-workers at Tohoku University, Sendai, Japan, 1979–1981. Portions of this work were presented at the symposium on "Electrochemical and Spectrochemical Studies of Biological Redox Components" at the 181st National Meeting of the American Chemical Society, Atlanta, GA, April 1981.

Registry No. Fe^{III}TMPyP, 60489-13-6; Fe^{II}TMPyP, 71794-64-4; H_2O_2, 7722-84-1; O_2, 7782-44-7; H_2O, 7732-18-5; TPyP, 16834-13-2.

Contribution from the Department of Chemistry, Brookhaven National Laboratory, Upton, New York 11973

Reactions of Tris- and Bis(2,2′-bipyridine)rhodium(II) Complexes in Aqueous Solution

HAROLD A. SCHWARZ* and CAROL CREUTZ*

Received July 9, 1982

Pulse-radiolytic methods have been used to characterize $Rh(bpy)_3^{2+}$ and $Rh^{II}(bpy)_2(aq)$. The rhodium(II) complexes are produced by one-electron reduction of $Rh(bpy)_3^{3+}$ and $Rh(bpy)_2(OH)_2^+$, respectively, by either e_{aq}^- or R· = $(CH_3)_2\dot{C}OH$ (the radical produced predominantly by the reaction of 2-propanol with the hydroxyl radical). For reduction by R·, rate constants of 2.3×10^9 M^{-1} s^{-1} for $Rh(bpy)_3^{3+}$ and 2.4×10^8 M^{-1} s^{-1} for $Rh(bpy)_2(OH)_2^+$ at 25 °C were found. Small amounts of "double reduction" give $Rh(bpy)_3^+$, which undergoes bipyridine dissociation with $k = 5 \times 10^4$ s^{-1} at 25 °C. The bis complex $Rh^{II}(bpy)_2(aq)$ exhibits two dissociable protons implicating pK_a ($Rh(bpy)_2(H_2O)_2^{2+}$–$Rh(bpy)_2(H_2O)(OH)^+$) = 8.6 and pK_a ($Rh(bpy)_2(H_2O)(OH)^+$–$Rh(bpy)_2(OH)_2^0$ = 11.1. In the absence of added bpy or $Rh(bpy)_3^{3+}$, $Rh^{II}(bpy)_2$ undergoes rapid dimerization ($k = (2.3 \times 10^{11})$ $\exp(-4.3$ kcal $mol^{-1}/RT)$ at pH 8.9), and the dimer ultimately converts to $Rh(bpy)_2^+$ and $Rh(bpy)_2(OH)_2^+$ ($k = 0.9 \times 10^{-2}$ s^{-1} at 25 °C, 0.8×10^{-1} s^{-1} at 60 °C). Reaction of bipyridine with $Rh(bpy)_2(H_2O)_2^{2+}$ to give $Rh(bpy)_3^{2+}$ proceeds with $k = 0.3 \times 10^9$ M^{-1} s^{-1}, while for the reverse reaction $k = 0.6$ s^{-1} at 25 °C and 4.3 s^{-1} at 50 °C. Disproportionation of $Rh(bpy)_3^{2+}$ to $Rh(bpy)_2^+$ and $Rh(bpy)_3^{3+}$ proceeds via reduction of $Rh^{II}(bpy)_2$ by $Rh(bpy)_3^{2+}$ ($k = 3.0 \times 10^8$ M^{-1} s^{-1} at pH 8.9 and 25 °C).

Introduction

Monomeric d^7 complexes of second and third transition series metal centers are unstable with respect to dimerization to metal–metal-bonded species, to disproportionation to the $d^6 + d^8$ counterparts, or to both. Thus little information concerning the elementary coordination chemistry of these species is available. For the $4d^7$ center rhodium(II), exceptions include the ammines[1] $Rh(NH_3)_6^{2+}$ and $Rh(NH_3)_4^{2+}(aq)$ generated in pulse radiolysis of $Rh(NH_3)_6^{3+}$ and $Rh(dmgH)_2$ produced[2] by flash photolysis of $[Rh(dmgH)_2PPh_3]_2$ (dmgH is the monoanion of 2,3-butanedione dioxime or dimethylglyoxime), among others.[3] Our work with $Rh(bpy)_3^{2+}$ (bpy = 2,2′-bipyridine) and $Rh^{II}(bpy)_2$ originated because these complexes are implicated as intermediates in a water photoreduction system,[4-6] and we have continued[7,8] these studies in order to attain a greater understanding of the nature and reactivity of these species. Here we report results that lead to the conclusion that these complexes are six-coordinate but extremely substitution labile. Bis(bipyridine)rhodium(II) has an extremely high affinity for a third bipyridine molecule and for itself (dimer formation), but under all circumstances the rhodium(II) complexes eventually disproportionate to rhodium(I) and rhodium(III). Our observations on $Rh(bpy)_3^{2+}$ are in agreement with but are an extension of those recently reported by Mulazanni and co-workers.[9]

Experimental Section

The 2,2′-bipyridine complexes $[Rh(bpy)_3](ClO_4)_3$ and $[Rh(bpy)_2(H_2O)_2](ClO_4)_3$ were prepared as described in ref 6. In some experiments sulfate salts (as solutions) were used. These were prepared via anion exchange of the perchlorate salts.[6] Fischer Certified 2-propanol was used as obtained. Generally the solutions were 1.0% by volume 2-propanol (0.13 M). Reagent grade sodium phosphate and borate salts were used as buffers with the total buffer concentration being in the $(2–5) \times 10^{-3}$ M range. Milli-Q water was used in all the solutions, and argon was the blanket gas.

Pulse radiolysis was carried out with 2-MeV electrons produced by a Van de Graaff accelerator. The pulse lengths were varied but were usually in the range of 0.2–3 μs, and the electron currents ranged up to 0.4 A. The electron beam passed through the 0.5-cm dimension and the analyzing light through the 2-cm dimension of a $2 \times 1 \times 0.5$ cm Supersil cell. The light passed through the cell one or three times for path lengths of 2 or 6 cm. The light was produced by a Xe arc when time periods shorter than 10^{-4} s were studied and by a quartz–iodine lamp (above 400 nm) or a D_2 arc (below 400 nm) for longer periods. The D_2 arc could be pulsed to increase its output a factor of 8 for periods up to 5 ms. The cell was thermostated between 5 and 75 °C with most work done at 25 °C.

Results

Production of Rhodium(II) Complexes. The radiolysis of aqueous solutions produces hydroxyl radicals, hydrated electrons, and hydrogen atoms in the ratios 2.8:2.7:0.6. Some

(1) Lilie, J.; Simic, M. G.; Endicott, J. F. *Inorg. Chem.* **1975**, *14*, 2129.
(2) Tinner, U.; Espenson, J. H. *J. Am. Chem. Soc.* **1981**, *103*, 2120.
(3) Felthouse, T. R. *Prog. Inorg. Chem.* **1982**, *29*, 73.
(4) Kirch, M.; Lehn, J. M.; Sauvage, J. P. *Helv. Chim. Acta* **1979**, *62*, 1345.
(5) Brown, G. M.; Chan, S.-F.; Creutz, C.; Schwarz, H. A.; Sutin, N. *J. Am. Chem. Soc.* **1979**, *101*, 7638.
(6) Chan, S.-F.; Chou, M.; Creutz, C.; Matsubara, T.; Sutin, N. *J. Am. Chem. Soc.* **1981**, *103*, 369.
(7) Creutz, C.; Keller, A. D.; Schwarz, H. A.; Sutin, N. *ACS Symp. Ser.* **1982**, *198*, 382.
(8) Creutz, C.; Keller, A. D.; Sutin, N.; Zipp, A. P. *J. Am. Chem. Soc.* **1982**, *104*, 3618.
(9) Mulazzani, Q. G.; Emmi, S.; Hoffman, M. Z.; Venturi, M. *J. Am. Chem. Soc.* **1981**, *103*, 3362.

0020-1669/83/1322-0707$01.50/0